



ELSEVIER

Available online at www.sciencedirect.com

SCIENCE @ DIRECT®

Optics Communications 226 (2003) 377–386

OPTICS
COMMUNICATIONS

www.elsevier.com/locate/optcom

Relativistic laser harmonic generation from plasmas with density ripple

K.P. Singh ^{a,*}, V.L. Gupta ^b, V.K. Tripathi ^a

^a Department of Physics, Indian Institute of Technology, New Delhi 110016, India

^b Department of Electronic Science, University of Delhi, New Delhi 110021, India

Received 19 June 2002; received in revised form 10 January 2003; accepted 10 July 2003

Abstract

A high intensity laser obliquely incident on an underdense plasma with density ripple produces resonant second and third-harmonic radiation in the reflected component. The highest efficiency of harmonic generation occurs when the pump laser is incident at critical angle and the angle between ripple wave vector \mathbf{q} and the surface normal has a specific value $\phi = \phi_m$, at which phase-matching condition is satisfied. As the electron density varies from low densities to critical density, value of ϕ_m varies from 90° to 45° for second-harmonic and from 110° to 60° for third-harmonic. The efficiency of phase-matched harmonic generation is an order of magnitude higher than the efficiency without phase-matching. The intensity of second and third-harmonic is proportional to square and cube of laser intensity respectively, when $a_0 \ll 1$ and proportional to laser intensity when $a_0 \gg 1$, where a_0 is the normalized electric field parameter of the pump wave. © 2003 Elsevier B.V. All rights reserved.

1. Introduction

The interaction of intense short pulse lasers with plasmas leading to harmonic generation has been an active area of research in recent years (for review, see [1]). With the development of the chirped-pulse-amplification technique, table-top high-peak power lasers have been successfully developed. By focusing these laser pulses, the laser intensity can exceed 10^{19} W/Cm². At such intensities, motion of electrons becomes relativistic. Theory for coherent emission in the direction of propagation of laser beam, referred to as relativistic harmonic generation, has been derived [2,3]. It indicates that because of the mismatch between the phase velocities of the laser pulse and the generated harmonics and because of the collective response of the plasma, the conversion efficiency should be low unless a means for phase-matching [4] is implemented. Matsumoto and Tanaka [5] have presented analysis of quasi phase-matched second-harmonic generation in the reflection by backward propagating interaction and showed that bistability appears in the generated

* Corresponding author.

E-mail address: k_psingh@yahoo.com (K.P. Singh).

second-harmonic power if the amount of phase mismatch is suitably chosen. Experimentally, Liu et al. [6] tried to measure the third-harmonic light produced from relativistic harmonic generation but ultimately could give only an upper limit on the conversion efficiency. Meyer and Zhu [7] claimed to have observed the second relativistic harmonic generated under the condition of beam filamentation. However, such second-harmonic light has been later identified by several groups [8,9] to be associated with the transverse-density depression derived by laser self-channeling or filamentation, as is evident from its broad angular width caused by the plasma density gradient [7]. Shibu and Tripathi [10] have studied phase-matched third-harmonic generation of a laser beam propagating through a plasma channel and showed that the presence of a background density perturbation can account for phase-matching. Parashar and Pandey [11] have proposed a scheme of efficiency enhancement of second-harmonic by introducing a density ripple into the interaction region. Ripple provides the additional momentum required by the second-harmonic for phase-matching. Rax et al. [12] have analyzed relativistic second-harmonic generation with ultrahigh intensity laser pulses in a weakly magnetized plasma. They addressed important issues of phase-matching, pump depletion, and relativistic tapering considering both permanent magnet and laser driven wigglers. They found that wiggler magnetic field plays both a dynamical role in producing the traverse harmonic current and a kinematical one in ensuring phase-matching. Yang et al. [13] have observed strong third-harmonic emission with a conversion efficiency higher than 0.1% from a plasma channel formed by self-guided femtosecond laser pulses propagating in air. They found an optimized condition under which the third-harmonic conversion efficiency is maximized. Their experimental results show that radiation of the emission in ultraviolet wavelength range makes a major attribution to third-harmonic emission, whereas the effects of self-phase modulation are not important when intense laser pulses interact with gaseous media. Recently, Chen et al. [15] have experimentally observed phase-matched relativistic third-harmonic generation, angular pattern of which being a forward directed cone and the signal level being on the same order of magnitude for circularly polarized pump pulse as for a linearly polarized pump pulse.

To meet the challenge of high-power, short wavelength coherent radiation generation, it is quite interesting to identify an efficient frequency conversion scheme. In this paper we study second and third-harmonic generation by an obliquely incident laser on a vacuum–plasma interface. The plasma density is taken underdense ($n_0^0 < n_{cr}$) with a density ripple $n_q = n_q^0 e^{+iq(\sin \phi x + \cos \phi z)}$, where n_0^0 , n_{cr} and n_q^0 are the plasma density, critical density and ripple density, respectively, and ϕ is the angle between ripple vector \mathbf{q} and z -axis. The laser of frequency ω induces an oscillatory velocity \mathbf{v}_1 on electrons at (ω, \mathbf{k}) and exerts a $\mathbf{v}_1 \times \mathbf{B}_1$ ponderomotive force on electrons at $(2\omega, 2\mathbf{k})$. The ponderomotive force and self-consistent field \mathbf{E}_2^+ induce oscillatory velocities \mathbf{v}_2 and \mathbf{v}_2^+ on electrons at $(2\omega, 2\mathbf{k})$ and $(2\omega, 2\mathbf{k} + \mathbf{q})$ which couple with n_q and n_0^0 , respectively, to produce a second-harmonic current and density oscillations n_2^+ at $(2\omega, 2\mathbf{k} + \mathbf{q})$. The density oscillations n_2^+ couple with \mathbf{v}_1 to produce a third-harmonic nonlinear current at $(3\omega, 3\mathbf{k} + \mathbf{q})$. The currents at second and third-harmonic create space charge oscillations on the plasma surface and give rise to electromagnetic second and third-harmonic radiation in the reflected component. The model is valid for underdense plasma, angle of incidence varying from 0° to the critical angle. Beyond critical angle propagation vector becomes imaginary and the laser propagation becomes evanescent.

2. Harmonic current density

Consider a vacuum–plasma interface at $z = 0$, $z < 0$ being vacuum and $z > 0$ a plasma with a density ripple $n_q = n_q^0 \exp[+iq(\sin \phi x + \cos \phi z)]$. A laser polarized in the plane of incidence is incident on the interface at an angle of incidence θ (cf. Fig. 1).

$$\mathbf{E}_{1i} = (\hat{x} \cos \theta - \hat{z} \sin \theta) E_{10} \cos(\omega t - k_x x - k_{0z} z), \quad (1)$$

where $k_x = (\omega/c) \sin \theta$ and $k_{0z} = (\omega/c) \cos \theta$.

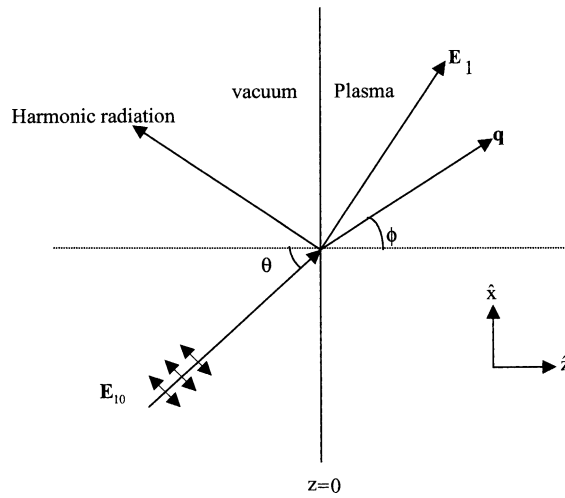


Fig. 1. Schematic of harmonic generation process.

Inside the plasma the electric and magnetic fields of the transmitted laser can be written as

$$\mathbf{E}_1 = ((\epsilon_1 - \sin^2 \theta)^{1/2} \hat{x} - \sin \theta \hat{z}) E_1 \cos(\omega t - k_x x - k_z z), \tag{2}$$

$$\mathbf{B}_1 = c \mathbf{k} \times \mathbf{E}_1 / \omega. \tag{3}$$

$a_1 = eE_1/m_0\omega c$, $a_0 = eE_{10}/m_0\omega c$, transmission coefficient $t_p = 2\epsilon_1^{0.5}/(\epsilon_1 + k_z/k_0z)$, $k_z = (\omega^2/c^2 \epsilon_1 - k_x^2)^{1/2}$, $\epsilon_1 = 1 - \omega_p^2/\omega^2$, relativistic plasma frequency $\omega_p^2 = 4\pi n_0^0 e^2/\gamma m_0$, where e , m_0 and γ are electronic charge, rest mass and average value of relativistic factor, respectively.

The equations governing electron momentum and energy are

$$\frac{dP_x}{dt} = -eE_1((\epsilon_1 - \sin^2 \theta)^{1/2} - \epsilon_1 v_z/c) \cos(\omega t - k_x x - k_z z), \tag{4}$$

$$\frac{dP_z}{dt} = eE_1(\sin \theta - \epsilon_1 v_x/c) \cos(\omega t - k_x x - k_z z), \tag{5}$$

$$\frac{d\gamma_t}{dt} = -\frac{eE_1}{m_0\omega c} (k_z v_x - k_x v_z) \cos(\omega t - k_x x - k_z z). \tag{6}$$

Using Eqs. (4)–(6) we obtain

$$\frac{d}{dt} \left\{ \frac{\hat{x}P_x + \hat{z}P_z}{m_0c} - c\gamma_t \frac{\mathbf{k}}{\omega} + a((\epsilon_1 - \sin^2 \theta)^{1/2} \hat{x} - \sin \theta \hat{z}) \sin(\omega t - k_x x - k_z z) \right\} = 0,$$

$$\frac{\hat{x}P_x + \hat{z}P_z}{m_0c} - c\gamma_t \frac{\mathbf{k}}{\omega} + a((\epsilon_1 - \sin^2 \theta)^{1/2} \hat{x} - \sin \theta \hat{z}) \sin(\omega t - k_x x - k_z z) = C_1,$$

where C_1 is a constant. If the electron is at the rest at origin in the beginning, then

$$C_1 = -\mathbf{k}c/\omega,$$

$$\frac{\hat{x}P_x + \hat{z}P_z}{m_0c} = c(\gamma_t - 1) \frac{\mathbf{k}}{\omega} + a_1((\epsilon_1 - \sin^2 \theta)^{1/2} \hat{x} - \sin \theta \hat{z}) \sin(\omega t - k_x x - k_z z). \tag{7}$$

When the electrons are accelerated, a space charge is created which neutralizes the term $c(\gamma_t - 1)\mathbf{k}/\omega$, therefore from Eq. (7), we obtain

$$\frac{P_x^2 + P_z^2}{m_0^2 c^2} = \varepsilon_1 a_1^2 \sin^2(\omega t - k_x x - k_z z). \quad (8)$$

Using Eq. (8) with $\gamma_t^2 = 1 + (P_x^2 + P_z^2)/m_0^2 c^2$, we obtain

$$\gamma_t = \{1 + a_1^2 \sin^2(\omega t - k_x x - k_z z) \varepsilon_1\}^{1/2}.$$

Time averaged value of relativistic factor

$$\gamma = \{1 + a_1^2 \varepsilon_1 / 2\}^{1/2}. \quad (9)$$

The electron velocity at (ω, \mathbf{k}) ,

$$\mathbf{v}_1 = \frac{e\mathbf{E}_1}{\gamma m_0 i\omega}. \quad (10)$$

The oscillating current at (ω, \mathbf{k}) ,

$$\mathbf{J}_1 = -n_0^0 e \mathbf{v}_1 = -\frac{n_0^0 e^2 \mathbf{E}_1}{\gamma m_0 i\omega}.$$

Using Maxwell's equations, we write

$$\nabla \times \mathbf{B} = \frac{4\pi}{c} \mathbf{J}_1 + \frac{1}{c} \frac{\partial \mathbf{E}_1}{\partial t} = -\frac{i\omega}{c} \left[1 - \frac{\omega_p^2}{\omega^2} \right] \mathbf{E}_1,$$

it gives electromagnetic wave dispersion relation

$$k^2 = \frac{\omega^c}{c^2} \left(1 - \frac{\omega_p^2}{\omega^2} \right). \quad (11)$$

\mathbf{v}_1 beats with \mathbf{B}_1 to produce the ponderomotive force \mathbf{F}_2 at $(2\omega, 2\mathbf{k})$,

$$\mathbf{F}_2 = \frac{i\mathbf{k}c\varepsilon_1 e}{2\gamma\omega} a_1 E_1 \exp[-i(2\omega t - 2k_x x - 2k_z z)]. \quad (12)$$

The electron velocity due to \mathbf{F}_2 and the self-consistent field \mathbf{E}_2 at $(2\omega, 2\mathbf{k})$ is

$$\mathbf{v}_2 = \frac{e\mathbf{E}_2 - \mathbf{F}_2}{2\gamma m_0 i\omega}. \quad (13)$$

The electron velocity due to the self-consistent field \mathbf{E}_2^+ at $(2\omega, 2\mathbf{k}+\mathbf{q})$ is

$$\mathbf{v}_2^+ = \frac{e\mathbf{E}_2^+}{2\gamma m_0 i\omega}. \quad (14)$$

Using Eqs. (12) and (13) in the equations of continuity $\partial n_2 / \partial t + \nabla \cdot (n_0^0 \mathbf{v}_2) = 0$ and $\partial n_2^+ / \partial t + \nabla \cdot (n_q \mathbf{v}_2 + n_0^0 \mathbf{v}_2^+) = 0$, respectively, we get the oscillatory electron densities n_2 and n_2^+ at the second-harmonic

$$n_2 = -\frac{n_0^0 (e\nabla \cdot \mathbf{E}_2 - \nabla \cdot \mathbf{F}_2)}{4\gamma m_0 \omega^2}, \quad (15)$$

$$n_2^+ = -\frac{\nabla \cdot [n_0^0 e \mathbf{E}_2^+ + n_q (e \mathbf{E}_2 - \mathbf{F}_2)]}{4\gamma m_0 \omega^2}. \tag{16}$$

Using n_2 and n_2^+ in Poisson’s equations $\nabla \cdot \mathbf{E}_2 = -4\pi e n_2$ and $\nabla \cdot \mathbf{E}_2^+ = -4\pi e n_2^+$, respectively, we obtain

$$\nabla \cdot \mathbf{E}_2 = \frac{ck^2 \varepsilon_1 \omega_p^2}{4\gamma \omega^3 \varepsilon_2} a_1 E_1 \exp[-i(2\omega t - 2k_x x - 2k_z z)], \tag{17}$$

$$\nabla \cdot \mathbf{E}_2^+ = \frac{c[\mathbf{k} \cdot (2\mathbf{k} + \mathbf{q})] \varepsilon_1 \omega_p^2 n_q^0}{8\gamma \varepsilon_2 \omega^3 n_0^0} a_1 E_1 \exp[-i(2\omega t - (2\mathbf{k} + \mathbf{q}) \cdot \mathbf{r})], \tag{18}$$

where $\varepsilon_2 = 1 - \omega_p^2/4\omega^2$ is the effective plasma permittivity at 2ω . Total current density at the second-harmonic is given by $-n_0^0 e v_2^+ - n_q e \mathbf{v}_2$,

$$\mathbf{J}_2^+ = -\frac{\omega_p^2 \mathbf{E}_2^+}{8\pi i \omega} + \frac{ck \varepsilon_1 \omega_p^2 n_q^0}{16\pi \gamma \varepsilon_2 \omega^2 n_0^0} a_1 E_1 \exp[-i(2\omega t - (2\mathbf{k} + \mathbf{q}) \cdot \mathbf{r})]. \tag{19}$$

The nonlinear current density at the third-harmonic is $\mathbf{J}_3^{\text{NL}} = -\frac{1}{2} n_2^+ e \mathbf{v}_1$,

$$\mathbf{J}_3^{\text{NL}} = ((\varepsilon_1 - \sin^2 \theta)^{1/2} \hat{x} - \sin \theta \hat{z}) \frac{i\mathbf{k} \cdot (2\mathbf{k} + \mathbf{q}) c^2 \varepsilon_1 \omega_p^2 n_q^0}{64\pi \varepsilon_2 \gamma \omega^3 n_0^0} a_1^2 E_1 \exp[-i(3\omega t - (3\mathbf{k} + \mathbf{q}) \cdot \mathbf{r})]. \tag{20}$$

The self-consistent current density at 3ω is

$$\mathbf{J}_3^L = -\frac{\omega_p^2 \mathbf{E}_3}{4\pi 3i\omega}. \tag{21}$$

Total third-harmonic current density is

$$\mathbf{J}_3 = \mathbf{J}_3^L + \mathbf{J}_3^{\text{NL}}. \tag{22}$$

3. Second-harmonic power density

The wave equation governing the generation of second-harmonic is given by

$$\nabla^2 \mathbf{E}_2^+ + \frac{4\omega^2}{c^2} \varepsilon_2 \mathbf{E}_2^+ = -\frac{i\mathbf{K}(4\omega^2/c^2 - |2\mathbf{k} + \mathbf{q}|^2) c \varepsilon_1 \omega_p^2 n_q^0}{8\gamma \varepsilon_2 \omega^3 n_0^0} a_1 E_1 \exp[-i(2\omega t - (2\mathbf{k} + \mathbf{q}) \cdot \mathbf{r})]. \tag{23}$$

We solve Eq. (23) separately in plasma and vacuum

$$\begin{aligned} E_{2x} &= [A_2 e^{ik_{2z}z} - \alpha_2 a_1 E_1 \exp[i(2k_z + q \cos \phi)z]] \exp[-i(2\omega t - (2k_x + q \sin \phi)x)] \quad \text{for } z > 0, \\ &= A_{2r} \exp[-i(2\omega t - (2k_x + q \sin \phi)x + k_{2r}z)] \quad \text{for } z < 0, \end{aligned} \tag{24}$$

where

$$\begin{aligned} k_{2z}^2 &= \frac{4\omega^2}{c^2} \varepsilon_2 - (2k_x + q \sin \phi)^2, \quad k_{2r}^2 = 4\frac{\omega^2}{c^2} - (2k_x + q \sin \phi)^2 \quad \text{and} \\ \alpha_2 &= \frac{i \sin \theta \varepsilon_1 \omega_p^2 n_q^0 (4\omega^2/c^2 - |2\mathbf{k} + \mathbf{q}|^2)}{8\gamma \varepsilon_2 \omega^2 n_0^0 ((4\omega^2/c^2) \varepsilon_2 - |2\mathbf{k} + \mathbf{q}|^2)}. \end{aligned}$$

Using Eqs. (18) and (24), we can write

$$\begin{aligned}
 E_{2z} &= \left[-\frac{2k_x + q \sin \phi}{k_{2z}} A_2 e^{ik_{2z}z} - \frac{k_z}{k_x} \alpha_2 a_1 E_1 \exp[i(2k_z + q \cos \phi)z] \right] \exp[-i(2\omega t - (2k_x + q \sin \phi)x)] \quad \text{for } z > 0, \\
 &= A_{2r} \frac{2k_x + q \sin \phi}{k_{2r}} \exp[-i(2\omega t - (2k_x + q \sin \phi)x + k_{2r}z)] \quad \text{for } z < 0,
 \end{aligned} \tag{25}$$

$$\begin{aligned}
 B_{2y} &= \frac{c}{2\omega} \left[A_2 \frac{k_2^2}{k_{2z}} e^{ik_{2z}z} + [(2k_x + q \sin \phi)k_z/k_x - (2k_z + q \cos \phi)] \alpha_2 a_1 E_1 \exp[i(2k_z + q \cos \phi)z] \right] \\
 &\quad \times \exp[-i(2\omega t - (2k_x + q \sin \phi)x)] \quad \text{for } z > 0, \\
 &= -\frac{c}{2\omega} \frac{4\omega^2/c^2}{k_{2r}} A_{2r} \exp[-i(2\omega t - (2k_x + q \sin \phi)x + k_{2r}z)] \quad \text{for } z < 0.
 \end{aligned} \tag{26}$$

Applying the continuity of E_{2x} and B_{2y} , at $z=0$, we obtain

$$A_{2r} = \alpha_2 a_1 E_1 \left(\frac{k_{2r} \{k_2^2 + k_{2z} ((k_z/k_x) q \sin \phi - q \cos \phi)\}}{k_{2r} k_2^2 + 4\omega^2/c^2 k_{2z}} \right). \tag{27}$$

The ratio of the reflected second-harmonic power density $P_2 = c|A_{2r}|^2/8\pi$ to that of the fundamental power density $P_0 = cE_{10}^2/8\pi$ can be written as

$$\frac{P_2}{P_0} = \left| \left(\frac{(a_0 t_p^2 \alpha_2 k_{2r} \{k_2^2 + k_{2z} q ((k_z/k_x) \sin \phi - \cos \phi)\}}{k_{2r} k_2^2 + 4\omega^2/c^2 k_{2z}} \right)^2 \right|. \tag{28}$$

Using $\mathbf{k}_2 = 2\mathbf{q} + \mathbf{q}$, we get the value of q required for phase-matching

$$q = [-2k \cos(\phi - \theta) + \sqrt{4k^2 \cos^2(\phi - \theta) + 3\omega_p^2/c^2}].$$

4. Third-harmonic power density

The wave equation governing the generation of third-harmonic is given by

$$\nabla^2 \mathbf{E}_3 + \frac{9\omega^2}{c^2} \left(1 - \frac{\omega_p^2}{9\omega^2} \right) \mathbf{E}_3 = -3i\omega \frac{4\pi}{c^2} \mathbf{J}_3^{\text{NL}}. \tag{29}$$

Employing \mathbf{J}_3^{NL} from Eq. (20), we solve Eq. (29) separately in plasma and vacuum

$$\begin{aligned}
 E_{3x} &= (A_3 e^{ik_{3z}z} - \alpha_3 a_1^2 E_1 \exp[i(3k_z + q \cos \phi)z]) \exp[-i(3\omega t - (3k_x + q \sin \phi)x)] \quad \text{for } z > 0, \\
 &= A_{3r} \exp[-i(3\omega t - (3k_x + q \sin \phi)x + k_{3r}z)] \quad \text{for } z < 0,
 \end{aligned} \tag{30}$$

where

$$k_{3z}^2 = \frac{9\omega^2}{c^2} \left(1 - \frac{\omega_p^2}{9\omega^2} \right) - (3k_x + q \sin \phi)^2, \quad k_{3r}^2 = \frac{9\omega^2}{c^2} - (3k_x + q \sin \phi)^2$$

and

$$\alpha_3 = \frac{3\mathbf{k} \cdot (2\mathbf{k} + \mathbf{q}) \varepsilon_1 \omega_p^2 n_0^0}{16\varepsilon_2 \gamma^2 \omega^2 n_0^0 \left[\frac{9\omega^2}{c^2} \left(1 - \frac{\omega_p^2}{9\omega^2} \right) - |3\mathbf{k} + \mathbf{q}|^2 \right]}.$$

Using Eq. (30) in $\nabla \cdot \mathbf{E}_3 = 0$, we can write

$$\begin{aligned}
 E_{3z} &= \left(-\frac{3k_x + q \sin \phi}{k_{3z}} A_3 e^{ik_{3z}z} + \frac{3k_x + q \sin \phi}{3k_z + q \cos \phi} \alpha_3 a_1^2 E_1 \exp[i(3k_z + q \cos \phi)z] \right) \\
 &\quad \times \exp[-i(3\omega t - (3k_x + q \sin \phi)x)] \quad \text{for } z > 0, \\
 &= \frac{3k_x + q \sin \phi}{k_{3r}} A_{3r} \exp[-i(3\omega t - (3k_x + q \sin \phi)x + k_{3r}z)] \quad \text{for } z < 0.
 \end{aligned}
 \tag{31}$$

Applying the continuity of E_{3x} and E_{3z} at $z = 0$, we obtain

$$A_{3r} = \frac{k_{3r} \alpha_3 a_1^2 E_1}{3K_z + q \cos \phi} \left(\frac{k_{3z} - 3k_z - q \cos \phi}{k_{3z} + k_{3r}} \right).
 \tag{32}$$

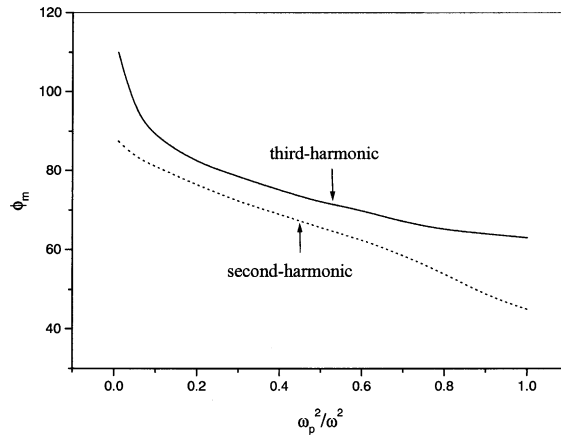


Fig. 2. Optimum value of angle ϕ_m as a function of normalized electron density ω_p^2/ω^2 at $a_0 = 3.0$.

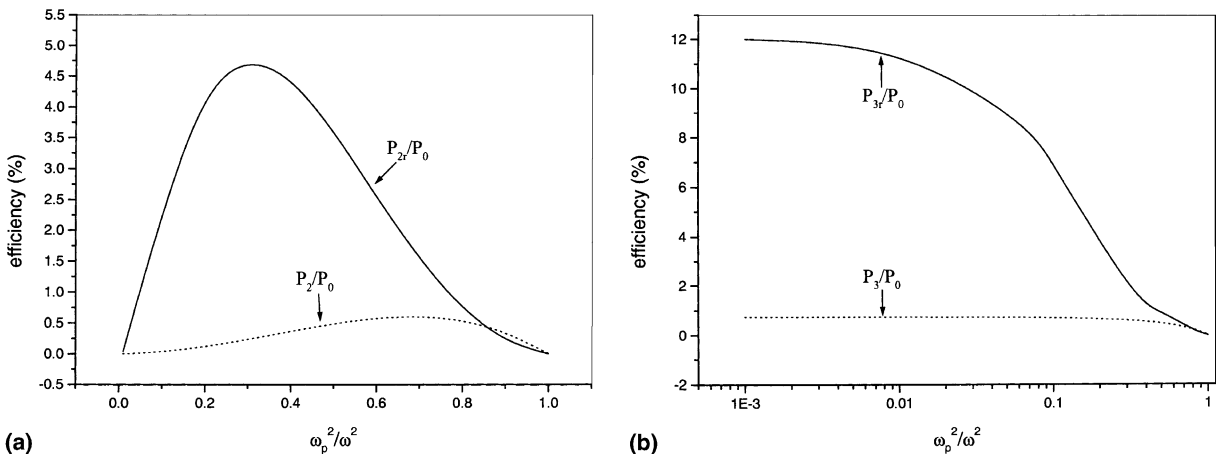


Fig. 3. (a) Efficiency of second-harmonic generation and (b) efficiency of third-harmonic generation as a function of normalized electron density ω_p^2/ω^2 at $a_0 = 3.0$.

The ratio of the reflected third-harmonic power density, $P_3 = c|A_{3r}|^2/8\phi$ to that of the fundamental power density $P_0 = cE_{10}^2/8\phi$ can be written as

$$\frac{P_3}{P_0} \left[\left[\frac{a_0^2 t_p^3 \alpha_3 k_{3r}}{3k_z + q \cos \phi} \frac{k_{3z} - 3k_z - q \cos \phi}{k_{3z} + k_{3r}} \right]^2 \right]. \tag{33}$$

Using $\mathbf{k}_3 = 3\mathbf{k} + \mathbf{q}$, we get the value of q required for phase-matching

$$q = [-3k \cos(\phi - \theta) + \sqrt{9k^2 \cos^2(\phi - \theta) + 8\omega_p^2/c^2}].$$

From Eqs. (24), (25), (30) and (31) we can observe second and third-harmonic radiations are p-polarized. Efficiency of second and third-harmonic generation peaks at critical angle of incidence. Results of Figs. 2–5 have been obtained at critical angle of incidence. Efficiency also depends on the angle ϕ

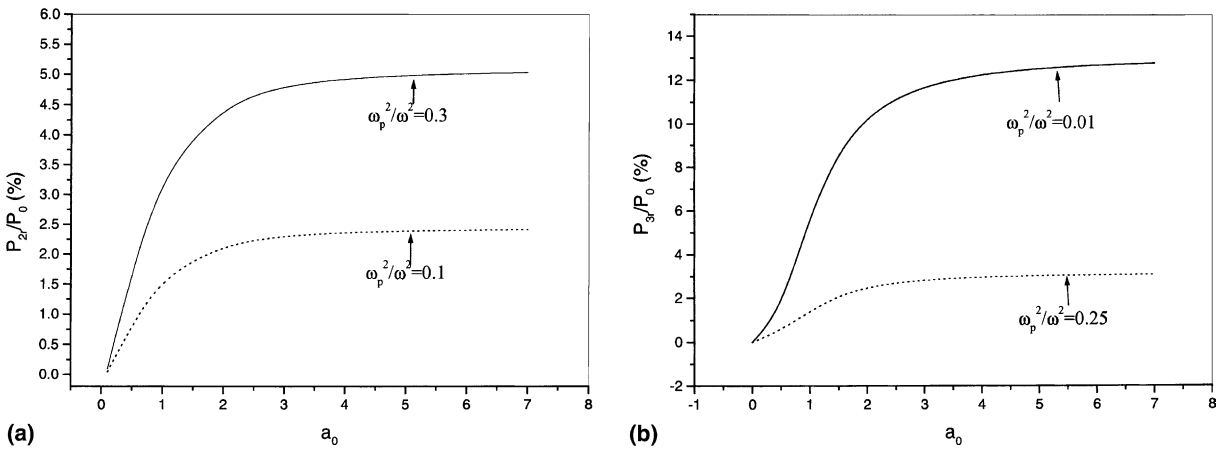


Fig. 4. (a) Resonant efficiency of second-harmonic generation at $\omega_p^2/\omega^2 = 0.1$ and $\omega_p^2/\omega^2 = 0.3$ and (b) resonant efficiency of third-harmonic generation at $\omega_p^2/\omega^2 = 0.01$ and $\omega_p^2/\omega^2 = 0.25$ as a function of normalized electric field parameter a_0 .

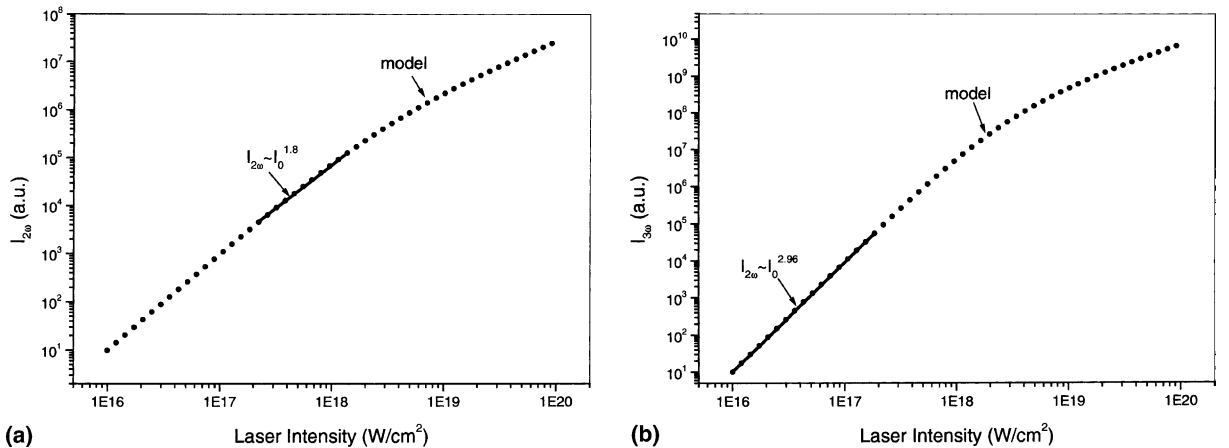


Fig. 5. (a) Resonant efficiency of second-harmonic generation at $\omega_p^2/\omega^2 = 0.3$ and (b) resonant intensity of third-harmonic at $\omega_p^2/\omega^2 = 0.01$ as a function of laser intensity I_0 .

and becomes maximum at an optimum value of the angle $\phi = \phi_m$. Fig. 2 shows variation of the angle ϕ_m as a function of normalized electron density at $a_0 = 3.0$. As ω_p^2/ω^2 varies from 0.01 to 1, ϕ_m varies from 90° to 45° for second-harmonic and from 110° to 60° for third-harmonic. Results of Figs. 3–5 have been obtained at optimum value of the angle ϕ and $n_q^0/n_0^0 = 0.1$. We call the efficiency at $\phi = \phi_m$ as resonant efficiency, P_{2r}/P_0 and P_{3r}/P_0 to distinguish these from the efficiency without any density ripple, P_2/P_0 and P_3/P_0 , respectively. In Fig. 3(a) and (b) we have plotted efficiency of second and third-harmonic generation as a function of ω_p^2/ω^2 at $a_0 = 3.0$. It can be observed that in the absence of any density ripple, maximum efficiency of second-harmonic generation is nearly 0.6% at $\omega_p^2/\omega^2 \cong 0.7$ and that of third-harmonic generation is nearly 0.75% at $\omega_p^2/\omega^2 \cong 0.01$.

When the plasma has an optimum density ripple, maximum efficiency of second and third harmonic generation is obtained at $\omega_p^2/\omega^2 \cong 0.3$ and $\omega_p^2/\omega^2 \cong 0.01$, respectively. Efficiency of phase-matched second and third-harmonic generation is nearly 10 and 16 times higher than the efficiency of corresponding harmonics without phase-matching. Fig. 4(a) and (b) show resonant intensity of second and third-harmonic generation as a function of normalized electric field parameter a_0 at different densities. Resonant efficiency of second and third-harmonic generation increases sharply in the non-relativistic regime, however, at higher intensities it saturates. Fig. 5(a) and (b) show variation of resonant intensity of second and third-harmonic (a.u.) as a function of laser intensity at $\omega_p^2/\omega^2 \cong 0.3$ and $\omega_p^2/\omega^2 \cong 0.01$, respectively. Intensity of second and third-harmonic is proportional to laser intensity with a power of slightly less than 2 and 3, respectively, at low intensities and tends proportional to laser intensity at high intensities.

5. Discussion

A p-polarized high power laser obliquely incident on underdense plasma undergoes second and third-harmonic generation. Polarization of the second and third-harmonic radiation is given by \mathbf{J}_2 and \mathbf{J}_3 , respectively; therefore harmonic radiation is p-polarized for both the harmonics. Intensity of the second and third-harmonic is proportional to $|\mathbf{J}_2^+|^2$ and $|\mathbf{J}_3^+|^2$, respectively, therefore efficiency of both the harmonics tends to zero as electron density approaches critical density and increases with the increase in normalized electron density for second-harmonic (Fig. 3) at low electron densities $|\mathbf{J}_2^+|^2$ and $|\mathbf{J}_3^+|^2$ are proportional to a_0^4/γ^2 and a_0^6/γ^4 , respectively, where $\gamma = (1 + a_0^2/2)^{0.5}$. In the non-relativistic regime term a_0^2 is not significant and the intensity of second and third-harmonic is proportional to laser intensity with a power of slightly less than 2 and 3, respectively, however, in relativistic regime a_0^2 becomes significant and intensity tends to proportional to laser intensity in the strong relativistic regime for both the harmonics. The intensity of the second and third-harmonic is proportional to laser intensity with a power of 1.8 and 2.96 for laser intensity varying from 2.5×10^{17} to 1.3×10^{18} W/cm² and from 10^{16} to 2×10^{17} W/cm² respectively. Takahashi and coworkers [14] and Chen et al. [15] have experimentally studied second and third-harmonic generation, respectively, and observed same scales of intensity dependence for the ranges stated above but under different geometries and conditions than that of ours.

The presence of density ripple provides extra momentum $\hbar q$ to the harmonic photon. Process of harmonic generation becomes resonant when electron density ripple of suitable wavelength is present in the plasma. One may launch a sound wave in the plasma with a ripple wave number q comparable to k to produce density ripple. The sound wave can be generated internally via Brillouin scattering of EM waves.

Acknowledgements

One of the authors, K.P. Singh, was supported by CSIR, Govt. of India.

References

- [1] P. Gibbon, *IEEE J. Quantum Electron.* 33 (1997) 1915.
- [2] E. Esarey et al., *IEEE Trans. Plasma Sci.* 21 (1993) 95.
- [3] W.B. Mori, C.D. Decker, W.P. Leemans, *IEEE Trans. Plasma Sci.* 21 (1993) 110.
- [4] J.M. Rax, N.J. Fisch, *IEEE Trans. Plasma Sci.* 21 (1993) 105.
- [5] M. Matsumoto, K. Tanaka, *IEEE J. Quantum Electron.* 31 (1995) 700.
- [6] X. Liu, D. Umstadter, E. Esarey, A. Ting, *IEEE Trans. Plasma Sci.* 21 (1993) 90.
- [7] J. Meyer, Y. Zhu, *Phys. Fluids* 30 (1987) 890.
- [8] V. Malka et al., *Phys. Plasmas* 4 (1997) 1127.
- [9] K. Krushelnick, *Phys. Rev. Lett.* 75 (1995) 3681.
- [10] S. Shibu, V.K. Tripathi, *Phys. Lett. A* 99 (1998) 239.
- [11] J. Parashar, H.D. Pandey, *IEEE Trans. Plasma Sci.* 20 (1992) 996.
- [12] J.M. Rax, J. Robiche, I. Kostyukov, *Phys. Plasmas* 7 (2000) 1026.
- [13] H. Yang et al., *Phys. Rev. E* 67 (2003) 015401.
- [14] M. Mori, E. Takahashi, K. Kondo, *Phys. Plasmas* 9 (2002) 2818.
- [15] S.Y. Chen et al., *Phys. Rev. Lett.* 84 (2000) 5528.